



ThinPV research project

(Co-financed by CCEM-CH and swisselectric research)

Start: 1.4.2007

Evaluation period: 1.1.2009-30.11.2009

Cost efficient thin film photovoltaics for future electricity generation

CCEM Annual Report 2009

Project Coordinator: Dr. Frank Nüesch

Date: 17.12. 2009

swisselectric
research


ccem.ch

1. Introduction

ThinPV is an interdisciplinary project on thin film photovoltaics. It brings together Swiss scientists active in fundamental and applied research on the major thin film photovoltaic technologies; mc- and a-silicon, chalcogenide, dye sensitized and organic. The project also includes optical modelling of these thin film devices. Research objectives focus on high rate silicon deposition processes and novel hybrid device concepts. Additionally, yearly workshops and topical conferences are implemented within ThinPV to promote the exchange of knowledge and competences between the partners and to attract young scientists to the field of photovoltaics. The project has now been running for more than two years and has benefited from numerous scientific meetings as well as three workshops. The next ThinPV conference “Transparent conducting electrodes for photovoltaics” will take place on January 25th at the Stade de Suisse in Bern. More than 50 participants have already registered.

Important funding from the CCEM as well as from “swisselectric research” is gratefully acknowledged. As detailed in the Annual Report 2007 the project is divided into two parts, officially starting on the 1.7.2007 and 1.4.2007 for part A and B, respectively.

2. Short summary

Regarding the work on enhanced Si deposition processes and better control of large surface area plasma enhanced chemical vapour deposition (part A), the set of plasma diagnostic tools was further improved. In 2009 these tools were applied to process analyses and improvement. The major achievements include:

- The influence of non planar electrode geometries, in plasma deposition chambers have been investigated experimentally and theoretically to model real plasma chambers with screws, showerheads etc.. It was found that the presence of sharp edges at holes or cylinders had no significant influence on radio frequency electric field breakdown.
- First implementation of time-resolved measurements of absolute Silane concentration in Plasma Enhanced Chemical Vapour Deposition (PECVD) reactors and simultaneously in the surrounding chamber.
- Under typical process conditions, it was shown that—for a given deposition rate—powder can be an indicator of favourable process conditions.
- Based, on the various diagnostic tools, a reduction of the transients observed during the initial growth of the devices could be controlled by optical emission spectroscopy during deposition of microcrystalline cells. The efficiency of the reference microcrystalline cell could thus be improved from 7.1 to 7.6 %.

Regarding the development of hybrid tandem solar cells and cyanine solar cells (Part B) important results have been achieved:

- Monolithic tandem cell consisting of a DSC top cell and a CIGS bottom cell with 12% power conversion efficiency was fabricated.
- Hybrid tandem solar cell stability could be enhanced by introducing advanced protection layers on top of the CIGS cell.
- Numerical modelling and conversion efficiency calculation of monolithic hybrid tandem cells have been carried out.
- Preliminary estimation of power conversion efficiency in triple junction solar cells based on CIGS, CdTe and DSC junctions have been made.
- In organic solar cells based on cyanine dyes, high power conversion efficiencies from 3% to 4% could be achieved without requiring chemical doping of the cyanine layer. Red to near infrared absorbing squaraine dyes have been successfully implemented in bilayer organic solar cells.
- Extension of the optical device model by including charge transfer excitons. The influence of the coherence length of the incident light irradiation on the interference phenomena in thin layer organic solar cells has been investigated.
- A photo-CELIV (charge extraction by linearly increasing voltage) measurement has been installed in order to measure materials parameters for modelling purposes such as charge carrier mobility and lifetime.

Joint educational activities (Part C) will be further pursued. The last conference planned in the framework of the present *ThinPV* project will take place on January 25th 2010 at the Stade de Suisse in Bern. The workshop will focus on different possibilities to achieve highly transparent and conductive electrodes. The latter include doped oxides, dispersed carbon nanotubes, thin metal grids as well as fabric electrodes.

In order to continue and extend the exchange and common research activities between Swiss research laboratories in thin film photovoltaics, considerable effort has been dedicated in developing and submitting common research projects for the coming years. These projects include an NCCR (leading house EPFL), a CCEM (leading house Empa), as well as other more specific projects (CTI, EKZ) between the *ThinPV* partners.

3. Project timetable and advancement

The Gantt chart below gives an overview of the project advancement

Part A	Description	1Q1	1Q2	1Q3	1Q4	2Q1	2Q2	2Q3	2Q4	3Q1	3Q2	3Q3	3Q4
A1	Development of characterizatn tools	MA1	MA2		MA3								
A2	Review on process reliability						MA4						
A3	Evaluation of KAI reactor. Concept of an ideal PECVD reactor						MA5						
A4	Design and fabrication of new generation PECVD reactor								MA6				
A5	Tuning and optimization of the new PECVD reactor									MA7			MA8
A6	Development of new generation plasma process control tool												
Part B	Description	1Q1	1Q2	1Q3	1Q4	2Q1	2Q2	2Q3	2Q4	3Q1	3Q2	3Q3	3Q4
B1	First investigations on the hybrid tandem concept	MB1	MB2										
B2	Synthesis and tuning of the organic dyes/inorganic semiconductors				MB3								
B3	Optimization of the individual solar cell devices of the tandem cell						MB4						
B4	Development of monolithically integrated multijunction hybridsolar cells								MB5		MB6		
B5	Optimization and reliability of integrated multijunction hybrid solar cells												MB7
B6	Elaborate fabrication procedures of technological relevance												MB8
Part C	Description	1Q1	1Q2	1Q3	1Q4	2Q1	2Q2	2Q3	2Q4	3Q1	3Q2	3Q3	3Q4
C1	Implementation of other research groups to support activites of A or B		MC1		MC2								
C2	Organize relular meetings involving the project partners	MC3				MC4				MC5			
C3	Organization of workshops				MC6				MC7				MC8
Summary and Conclusions													S

MA1	Report on implementation of plasma analyses tools	End of 1Q1
MA2	Start of fabrication of analysis tools	End of 1Q1
MA3	Installation of electrical and optical diagnostic tools at CRPP	End of 1Q4
MA4	Report on parasitic phenomena in large KAI reactors	End of 2Q1
MA5	Report on new thin film structural and compositional analyses techniques	End of 2Q1
MA6	Design of ideal reactor completed	End of 2Q4
MA7	Installation of reactor	End of 3Q2
MA8	Characterization of micro cristalline Si layers and multijunction solar cells prepared in new reactor	End of 3Q4
MB1	Evaluation of a hybrid multijunction solar cell concept with ideal cell and material properties	End of 1Q1
MB2	Preliminary multijunction solar cells based on hybrid technology	End of 1Q2
MB3	Synthesis of the first materials required for optimized multijunction devices	End of 1Q4
MB4	Optimized multijunction solar cells based on hybrid technology	End of 2Q4
MB5	Installation of spray pyrolysis TCO coating equipment completed	End of 2Q4
MB6	Monolithical integration of multijunction solar cells	End of 3Q2
MB7	Optimized monolithically integrated multijunction solar cells	End of 3Q4
MB8	Concept for upscaling fabrication	End of 3Q4
MC1	Collaboration with a theory group to support part A or B	End of 1Q2
MC2	Define further collaborations	End of 1Q4
MC3	Kick-off meeting	End of 1Q1
MC4	General Assembly meeting	End of 2Q1
MC5	General Assembly meeting	End of 3Q1
MC6	Workshop to discuss the research needs of industry involved in thin film PV	End of 1Q4
MC7	Workshop with educational activity (mainly for PhD students)	End of 2Q4
MC8	Workshop/Event to be defined	End of 2Q4
S	Final report, summary, conclusions and outlook	End of 3Q4

Project advancement

Above achievements almost fully meet the previously determined milestones (it has to be noted that the official starting dates are 1.4.2007 and 1.7.2007 for Part A and B, respectively). Additional achievements in cyanine solar cells and theoretical modelling are not accounted for in above chart.

Numerous subproject meetings with the researchers involved in the project have taken place. A list of the most important meetings is given below (for more information refer to <http://thinpv.empa.ch>).

3rd Steering Committee Meeting

Place: Bern (ETH board), February 13th 2009

Participants: Frank Nüesch (Empa), Michael Grätzel (EPFL), Ayodhya Tiwari (Empa), Massimiliano Capezzali (EPFL, liaison to CCEM), Christophe Ballif (EPFL)

Agenda: Overview of project advancement. Brief summary of CCEM evaluation of January 15th. Third year extension of “swisselectric research” support to ThinPV. Future CCEM calls. Synergizing research in thin film photovoltaics.

Decisions: M. Capezzali will contact M. Paulus (swisselectric research) to discuss and support the third year extension of ThinPV by swisselectric research. F. Nüesch takes up contact with S. Nowak to discuss financial support of workshops and conferences by the SFOE. The partners will not apply for the new CCEM project on electrification of individual transportation. F. Nüesch will develop a new project idea with the partners to be submitted to the CCEM in fall. The next ThinPV conference topic shall focus on transparent electrodes for photovoltaics. M. Capezzali suggests organizing the conference at the Stade de Suisse in Bern.

Part A meetings

Jan-Dec: establishment by IMT and Oerlikon of a EU consortium for Production technologies. Large FP-7 program in negotiation.

Jan-Oct: Various direct contacts between IMT and CRRP on plasma simulations and effects of reactor geometry (Hollenstein, Howling, Bartlomé, Strahm, Buehlman-Cuony, Ballif) and design of electrodes.

August 25th, Utrecht, A. Howling (CRPP), C. Ballif, P. Buehlman-Cuony. Meeting during the ICANS conference on reactor design and testing of various hypothesis.

Others: June 25th: discussion on material qualities with A. Smets (AIST (jP) at IMT with Oerlikon Solar

Part B meetings

Place: Empa, May 15th 2009

Participants: Frank Nüesch (Empa), Bin Fan (Empa), Roland Hany (Empa), Fernando Castro (Empa), Sophie Wenger (Empa, Assistance / LPI, EPFL), David Brémaud (Thin Films and Photovoltaics Group, Empa), Sieghard Seyrling (Thin Films and Photovoltaics Group, Empa), Niels A. Reinke (ICP, ZHAW), Roger Häusermann (ICP, ZHAW), Daniele Rezzonico (Fluxim)

Agenda: Planned project continuation. Presentation and discussion of new results. Presentation of modeling software (SETFOS) by D. Rezzonico

Decisions: Join competences of Thin Films and Functional Polymers Groups (Empa), EPFL, and IMT to develop a stable protective intermediate layer for hybrid monolithic tandem solar cells. Optimize setup of mechanically stacked tandem to minimize electric losses at contacts. Set up an optical simulation of the stacked and monolithic tandem using the improved SETFOS software. For

this, the complex index of refraction (n and k) and the thickness of each layer must be known. EPFL is extracting the constants and modeling the DSC in collaboration with ZHAW (Gerbert Rüt Project). The model can be set up as soon as the input is known for the CIGS device.

Place: Empa, August 27th 2008

Participants: Frank Nüesch (Empa), Fan Bin (Empa), Jakob Heier (Empa), William Kylberg (Empa), Matthias Schmid (ICP, ZHAW), Jürgen Schumacher (ICP, ZHAW), Beat Ruhstaller (ICP, ZHAW), Nils A. Reinke (ICP, ZHAW), Daniele Rezzonico (FLUXIM)

Agenda: Use of Impedance spectroscopy in thin film photovoltaic device characterization.

Decisions: Power point presentations of the various contributions shall be made available to all partners.

Place: EPFL, November 24th 2009

Participants: Frank Nüesch (Empa), Bin Fan (Empa), Roland Hany (Empa), Sophie Wenger (Empa, Assistance / LPI, EPFL), Michael Grätzel (LPI, EPFL), Sieghard Seyrling (Thin Films and Photovoltaics Group, Thomas Lanz (ICP, ZHAW)

Agenda: Project advancement. Announcement of coming events/conferences. New results presented by the PhD students S. Wenger, S. Seyrling, Bin Fan.

Decisions: Empa (Functional Polymers) and EPFL: Impedance spectroscopy on cyanine-based organic solar cells and transient absorbance measurements of cyanine/C₆₀ to assess Schottky junction formation. Corrosion tests of various conducting polymers (spin-coat material on metal-coated glass, add a drop of iodine-based electrolyte). Test promising polymers in monolithic devices. Empa, EPFL, and ZHAW: Test various photovoltaic technologies with ZHAW home-built Photo-CELIV setup.

4. Main results achieved

Part A (EPFL; CRPP and IMT)

Understanding breakdown phenomena in plasma-enhanced chemical vapour deposition

One important use of plasma-enhanced chemical vapour deposition (PECVD) is the fabrication of thin-film transistor (TFT) displays and photovoltaic solar cells based on amorphous and micro-crystalline silicon. The substrates commonly used have grown from 350 mm x 450 mm in 1992 to 2850 mm x 3050 mm in 2007. This represents a 7-fold growth in diagonal, from half a meter to 4.17 metres, and an increase of surface area by a factor of 55! This demand for ever-larger substrates, coupled with new production techniques (e.g. the step from amorphous cells to amorphous-micro-crystalline cells) translates into progressively bigger RF power requirements.

Increasing the production area is unfortunately not as easy as up-scaling existing reactors and using more powerful generators. Non-linear effects have to be taken into account as the reactor dimensions reach a significant fraction of the RF wavelength, and parasitic plasmas as well as arcing can occur in power feed and showerheads. The latter effects can lead to a reduced lifetime, damaged or even destroyed reactors.

In PECVD-reactors small gaps are used between RF electrode and ground that are meant to prevent RF breakdown – predominantly in the showerhead (see Figure 1). These gaps can be, as a first approximation, considered as parallel plates with holes and/or elevations, and are supposed to be narrow enough to prevent a glow discharge, but wide enough to prevent metal-vapor arcing between the electrodes.

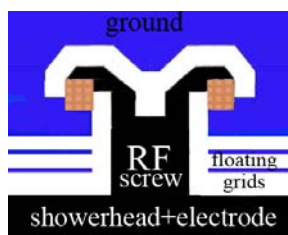


Figure 1: Small gaps and a ceramic ring (patterned) isolate the RF suspender screw from the ground potential of the reactor

These gaps have been shown to be vulnerable to damaging parasitic discharges when the reactor is used at higher powers and therefore higher RF voltages. While breakdown between parallel plates has been extensively treated in literature, irregular geometries are rarely mentioned. Accordingly, we investigated in the last year the behavior of breakdown in these non-parallel surfaces, with the aim of developing a basic understanding of the breakdown phenomenon and giving basic design rules for future reactor generations.

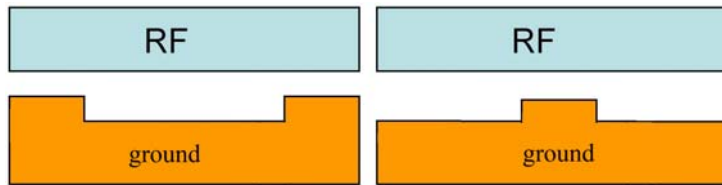


Figure 2: Cross section of the experimental setup. Hole electrode on the left, cylinder electrode on the right.

Experimental Setup

A typical experimental setup consisted in a flat cylindrical RF electrode, and separated from it by a gap of 4 mm a ground electrode with a 5 mm deep cylindrical hole, such that the distance between the bottom of the hole and the RF electrode was 9 mm. (see Figure 2, left). The diameter of the electrodes was 90 mm, and they were separated via Perspex-rings.

Another (earth) electrode used was a plate with a small 4mm diameter and 5 mm high cylinder in the middle (see Figure 2, right).

Results

Figure 3 shows some results of experiments with differing hole-radius. Each of the curves represents the breakdown RF voltage (peak to peak) over the pressure. It can be easily seen that the breakdown curves for all the hole-diameters fall between the two extrema of no hole (i.e. parallel plates with a 4 mm gap) and a hole the size of the electrode (i.e. parallel plates with a 9 mm gap). Furthermore, as the diameter of the holes increases from 4 mm to 60 mm, the curves steadily approach the limit of the case of two 9mm parallel plates.

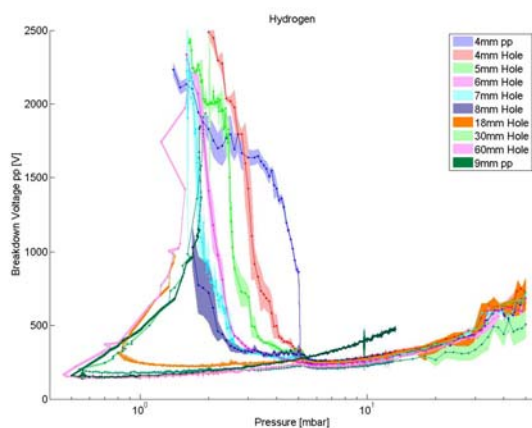


Figure 3: Breakdown curves for different hole-sizes in Hydrogen. The lines labelled "4mm pp" and "9mm pp" represent no hole and a hole-size equal to the electrode diameter, respectively.

This is surprising, since intuitively we expected sharp corners to strongly influence the breakdown voltage, i.e. lowering it considerably. Instead, the fact that the breakdown curves for electrodes with holes do not leave the 'envelope' presented by the extreme cases of 4 & 9 mm parallel plates indicates that breakdown in this kind of geometry does *not* happen at corners where the electric field is strongest, but rather depends on the maximum distance between the electrodes and on the radius of holes or hole-like structures (accounting for diffusive losses to the walls). Even a small hole, only 4 mm in diameter (light red in Figure 3) already shifts the steep left-hand branch of the breakdown curve to lower pressures. The bigger the diameter of the hole, the closer its breakdown curves resembles the one for parallel plates with nine millimetres separation.

Another series of electrodes, this time with protruding cylinders was tested. Figure 4 shows the resulting curve for a small cylinder of four millimetre diameter. At low pressures, the breakdown curve of the cylinder (in red) conforms to the breakdown curve for the case of parallel plates with nine millimetre separation. At higher pressures (above seven mbar), the influence of the small area of smaller gap on top of the cylinder comes into play, and the breakdown voltage is lower. Again it is clear that the higher field at the edge of the cylinder has no influence on the breakdown voltage, or else the breakdown curves would deviate noticeably from the parallel plate cases.

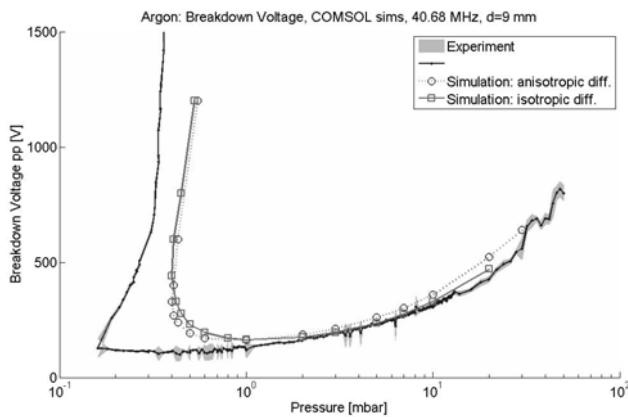


Figure 4: Breakdown curve in Hydrogen with cylinder electrode

Simulation

A fluid simulation was written, following the work of Lisovski. Argon swarm parameters were taken from the 1981 paper of Küçükarpaci. The simulation was written in the finite element solver COMSOL. A comparison with experimental results for parallel plates with nine millimetres separation in Argon is shown in figure 5. Secondary electron emission is not simulated, therefore the results do not agree with the experiment completely for the left-hand branch of the breakdown curve. The high-pressure right-hand branch however shows a reasonably good agreement between simulation and experiment.

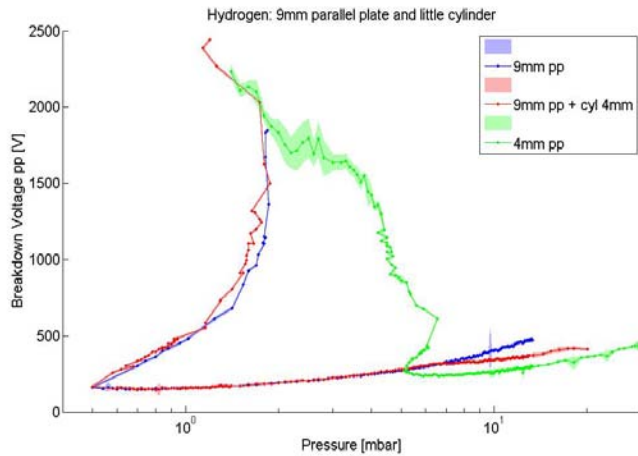


Figure 5: Experiment and Simulation of breakdown voltage

The simulation further confirms the hypothesis that the higher electric field at edges does not influence breakdown voltage. Figure 6 shows the electron density in the breakdown chamber at 5 and 0.8 mbar. Higher densities translate to brighter colours. The RF potential was applied to the top edge of the simulated region. The left edge is the symmetry axis, the bottom edge and the cylinder on the left are at ground potential, and the right edge is electric insulation (i.e. the Perspex rings). All borders are simulated as electron sinks (Electron density = 0). At five mbar (top of figure 6), the breakdown occurs in the smaller gap atop the cylinder on the left, while at 0.8 mbar (bottom of figure 6) the breakdown occurs in the wider gap to the right. The highest electric field would be right at the corner of the small cylinder (rounded with a radius of 0.1 millimeter), but clearly this has no perceptible effect on the electron density.



Figure 6: Numerical Simulation of electron density at a pressure of 5 mbar (left) and 0.8 mbar (right)

Future work will see the application of the fluid simulation to more complex geometries, like RF suspender screws and showerheads. With further experiments, including a suspender-screw analog, we hope to deepen our understanding of breakdown in irregular geometries. The effect of floating grids on the breakdown in a screw geometry will be tested as well.

Installation of electrical and optical diagnostic tools at CRPP and EPFL

In 2008 we reported the installation of three home-built optical diagnostic tools: an optical emission (OES) diagnostic tool, a laser light scattering (LLS) device to detect powder, and a quantum cas-

cade laser-based (QCL) absorption spectrometer to monitor silane. In 2009 we further developed the infrared laser spectrometer in order to acquire time-resolved measurements with a resolution of 40 ms. For this purpose we improved the temperature control and the wavelength stability of the QCL. With the help of time-resolved acquisitions, we studied the dynamic behavior of the silane density upon modification of input process conditions, or upon ignition of a plasma in the chemical vapor deposition (CVD) system.

Design and installation of an ideal reactor completed

In 2008 we reported the design and installation of a reactor with a reduced inter-electrode gap in order to increase the deposition rate. In 2009 we undertook further modifications to monitor the silane in the CVD system itself rather than in the pumping line of the system, as reported in 2008. The CVD system comprises the parallel-plate reactor and is surrounded by a chamber volume, which is separately pumped. In order to guide the mid-infrared laser beam through the CVD system, we replaced the lateral mesh of the reactor, the lateral viewports of the reactor, and the lateral viewports of the chamber. By mounting wedged viewport windows, we could monitor the first reflection of one reactor window, as illustrated in Fig 7. In this manner, the time-resolved SiH_4 density could be simultaneously measured in the reactor and the chamber of the PECVD system. Furthermore, the main mid-infrared laser beam was split in two to allow simultaneous measurements through the PECVD system and the pumping line.

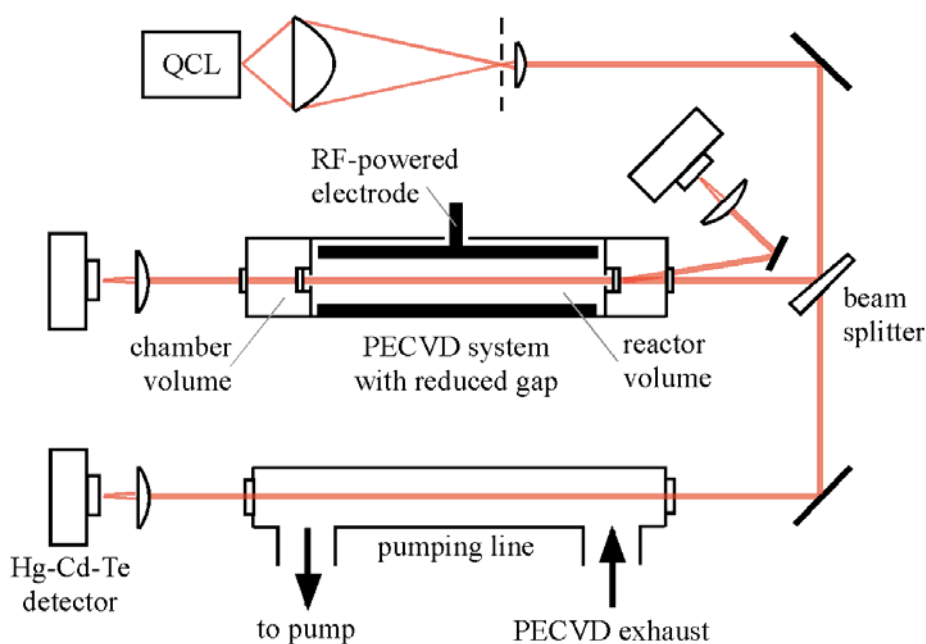


Figure 7. Experimental arrangement of the QCL-based absorption spectrometer and the PECVD system. Silane was monitored in the reactor volume, the chamber volume, and the pumping line.

In 2008 we confirmed that device-grade intrinsic microcrystalline ($\mu\text{c-Si:H}$) layers were associated with a low oxygen content and a preferential $\langle 220 \rangle$ crystallographic orientation, as often reported in literature. Such material is deposited in the so-called amorphous-to-microcrystalline transition regime. For depositions at a very-high-frequency of 40.68 MHz on p-doped $\mu\text{c-Si:H}$ layers heated at 453 K, it was found that the amorphous-to-microcrystalline transition regime corresponds to a silane concentration within the plasma between 1 and 2.8 %, as illustrated in Fig. 8a. Meanwhile, the formation of powder particles was monitored with the LLS device. In the absence of powder particles, we found that the film growth rate can be monitored in-situ based upon the measured silane dissociation and the input silane flow. As illustrated in Fig. 8b, the maximum achievable deposition rate in the ideal reactor is limited by the formation of powder particles.

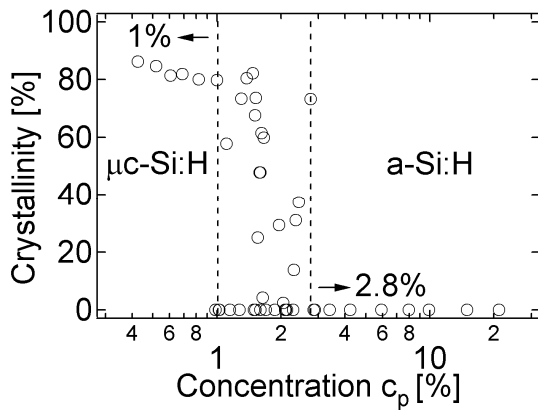


Figure 8a. Amorphous-to-microcrystalline Si transition. The silane concentration within the plasma, c_p , was measured with the infrared laser spectrometer, while the crystallinity was determined ex-situ by Raman spectroscopy.

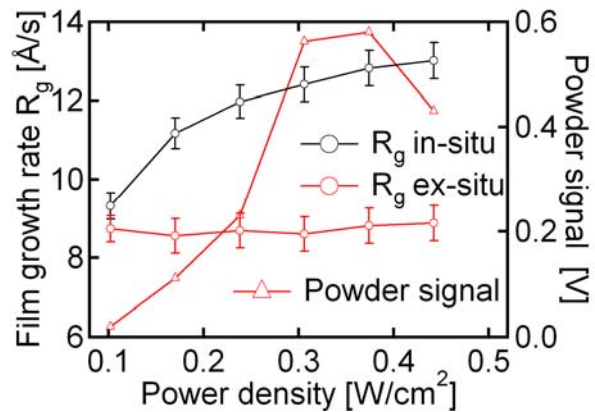


Figure 8b. Powder formation as a limiting factor in high-rate deposition of Si films. We measured in-situ the film growth rate, R_g , assuming that all dissociated SiH_4 contributes to the growth mechanism. The effective R_g was determined ex-situ following profilometric measurements.

We investigated the performance of microcrystalline cells grown at a high deposition rate of around 1 nm/s. In literature, the presence of powder is often regarded as a detrimental effect as it is associated with high deposition rates, where bulk material properties and cell performances degrade. Our results, however, show that—for a given deposition rate—powder is an indicator of favorable process conditions. This positive trend was investigated at a constant deposition rate and constant Raman crystalline fraction of 1 nm/s and 60%, respectively. During deposition, the presence of powder was monitored at the exhaust of the parallel-plate reactor with the LLS device (Fig. 9a), and within the plasma itself by OES (Fig. 9b). Both optical setups revealed similar trends. When the production of powder was the most significant (the H_2 flow was then set to 800 sccm), high-rate microcrystalline silicon solar cells had an efficiency of 7.1 %.

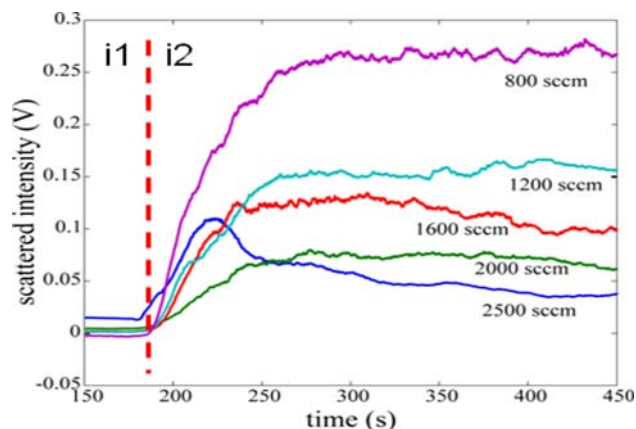


Figure 9a. Powder monitoring by LLS during deposition of Si solar cells.

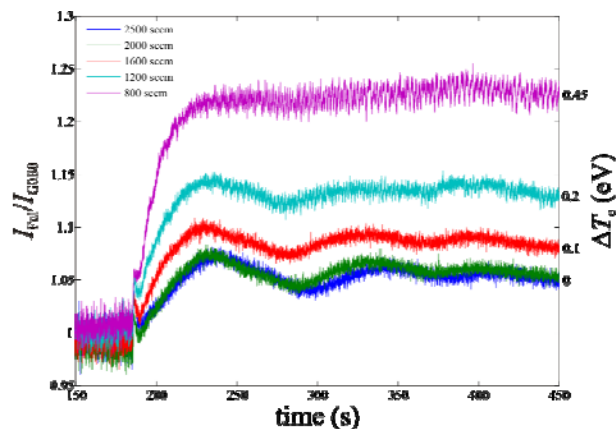


Figure 9b. Powder monitoring by OES during deposition of Si solar cells.

Following the bulk optimization described above, we studied plasma transients in order to optimize interfaces between successive layers of the device. With the help of our diagnostic tools, these transients could be attributed to artifacts other than the plasma dynamic itself, such as the reactor wall coverage, the use of a gas purifier and the initial capacitance value of the matching network, by means of which the radio-frequency power is coupled to the reactor cathode. Tailored processes were established to reduce plasma transients at the front contact/p-layer interface and at the p/i layer interface. The reduction of these transients was controlled by OES during deposition of microcrystalline cells; the efficiency of the reference cell could thus be improved from 7.1 to 7.6 %.

Outlook Part A

- For better understanding of PECVD operation in real vacuum chambers, fluid simulation to more complex geometries, like RF suspender screws and showerheads will be used. With further experiments, including a suspender-screw analog, we hope to deepen our understanding of breakdown in irregular geometries. The effect of floating grids on the breakdown in a screw geometry will be tested as well.
- While a considerable amount of effort has been undertaken to better understand the reactions taking place in chemical reactors, correlations between the plasma composition and device properties were cruelly lacking. Such correlations have now been established and will continue to be the target of future research.

Part B (LPI, EPFL; Thin Film and Photovoltaics Laboratory, Empa; Functional Polymers, Empa; ICP, ZHAW)

Monolithic DSC/CIGS Tandem Device with 12% Conversion Efficiency

Tandem solar cells using different bandgap absorbers allow efficient photovoltaic conversion in a wide range of the solar spectrum. The optical gaps of the dye-sensitized solar cell (DSC) and the Cu(In,Ga)Se₂ (CIGS) solar cell are ideal for application in double-junction devices. For the development of efficient and inexpensive tandem devices, monolithic integration of the two subcells is crucial to cut optical losses at needless interfaces and to reduce material costs. We have shown the feasibility of monolithic integration in 2008 with test devices reaching close to 10% efficiency. However, the performance of the device decreased rapidly due to corrosion of the bottom CIGS cell by the aggressive iodine-based electrolyte used in the top DSC. In 2009, by optimizing the front electrode of the CIGS cell, now using a 600 nm thick tin-doped indium oxide (ITO) layer instead of a 200 nm thick aluminum-doped zinc oxide (AZO) layer, the monolithic tandem device power conversion efficiency could be raised to 12% (Figure 1). The improvement was mainly due to a better fill factor, i.e. less shunt and series resistance losses at the junction between the two subcells. Even though the initial performance was higher due to a better protection of the bottom CIGS cell, degradation still occurred, probably due to infiltration of the electrolyte through pin-holes in the sputtered ITO layer. These results were reported in a peer-reviewed publication.

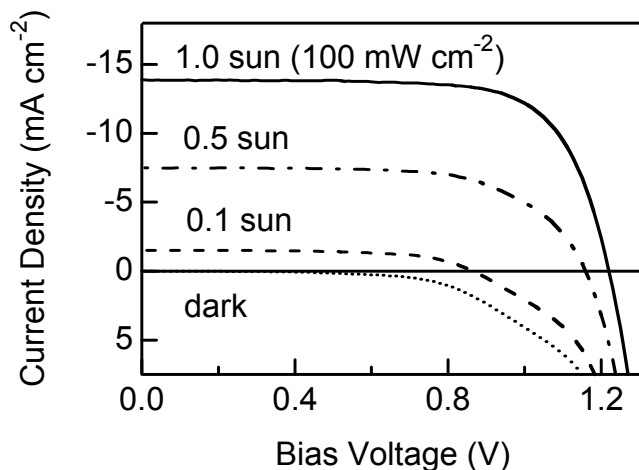


Figure 1. Current-voltage curve of a monolithic device under simulated solar radiation (AM 1.5G), reaching 12.2% at full sunlight. The curve in the dark shows nonideal rectification due to corrosion of the CIGS cell.

Improving Device Stability with Advanced Protective Layers

The influence of the DSC electrolyte on finished CIGS cells was investigated by applying a drop of electrolyte to the cell for about 40 min, then rinsing the cell and measuring the difference in IV behavior before and after electrolyte application. Even at such short exposure times the treatment re-

sulted in a significant decrease of cell performance, especially in the fill factor (Figure 2). As already outlined in the previous *ThinPV* report, SEM images showed that this degradation is caused by corrosion of the CIGS solar cell stack by the electrolyte, leading to short circuits between DSC and CIGS back contacts. Thus, the sum of the open circuit voltages between the two junctions is no longer observed and the PV characteristics are corresponding to those of the DSC alone.

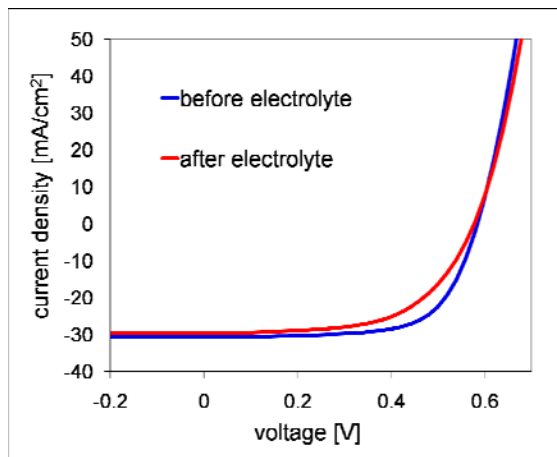


Figure 2: IV curves of a CIGS solar cell before and after 40 min of exposure to the iodide/tri-iodide electrolyte of a DSC.

To prevent degradation of the monolithic tandem device, a protective layer between the CIGS front electrode and the electrolyte must be developed, which is stable in the electrolyte environment, transparent in the wavelength range 600-1200 nm, and electrically conductive.

Fluorine-doped tin oxide (FTO) and tin-doped indium oxide (ITO) have proven to be stable in the electrolyte as they are frequently used as electrodes standard dye-sensitized solar cells. Zinc oxide (ZnO) is fairly stable in the electrolyte. With *Atomic Layer Deposition* (ALD), a chemical vapor deposition technique to produce conformal thin-films, these oxides can be deposited at ambient temperature on the CIGS electrode to fill up any cracks or pinholes. First tests were conducted with thin films (~10 nm, ZnO, TiO₂) deposited with a home-built ALD setup on glass coated with evaporated silver. Corrosion tests with a drop of electrolyte showed that the silver was attacked more slowly with a thin layer of ZnO. Monolithic tandem devices with an ADL-deposited ZnO intermediate layer showed a high open-circuit voltage (1.25 V) but an S-shaped current-voltage curve indicating that the ZnO layer is too insulating (Figure 3). The ZnO layer probably must be doped to ensure sufficient electrical conductivity. We are currently purchasing a state-of-the-art ADL system, with which we will be able to produce highly homogeneous, thick, and doped films.

Using spin-coated organic semiconductors as protective layer is alternative approach. So far, organic polymers could not be deposited satisfactorily since the CIGS electrode surface was not well wet by the polymer. Monolithic tandem devices with a polymer intermediate layer (PEDOT:PSS) showed no junction but a purely resistive behavior due to the thick and uneven polymer film. However, the wetting behavior might be improved by dissolving the polymer in a different solvent.

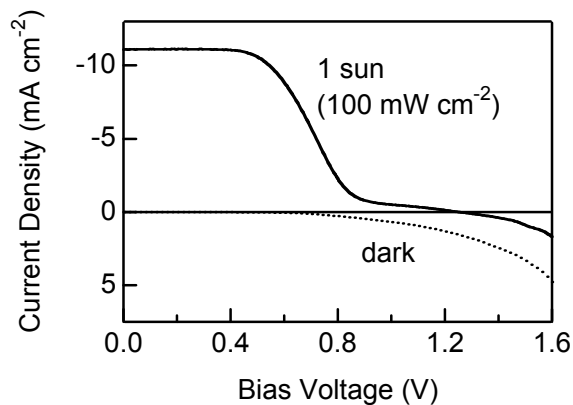


Figure 3. Current-Voltage curve under simulated solar radiation (AM 1.5G) of a monolithic device with a thin atomic layer deposited ZnO layer between the CIGS electrode and the electrolyte. The high open-circuit voltage (1.25 V) confirms the double junction between the subcells, but the S-shaped curve under full sunlight indicates an insulating behavior of the intermediate ZnO layer.

Understanding the optics in hybrid tandem devices using numerical modeling

Matching of the photocurrents in the top and bottom cell of a tandem device is crucial for efficient operation. The individual photocurrents cannot be measured in a monolithic tandem device since there are only two electric contacts between which one measures the current determined by the limiting subcell. However, the maximum photocurrent in the subcells can be calculated using coherent and incoherent optics to determine the light intensity in the absorbing films. The simulations can be done with commercial software, such as *SETFOS* (Fluxim, spin-off company of ZHAW). *SETFOS* is based on a multi-layer optical transfer matrix approach and requires the thickness and the complex index of refraction of each layer to calculate the total transmittance, reflectance, and the absorbance in each layer of the stack.

Simulations of transmittance and reflectance spectra were first calculated for the dye-sensitized solar cell alone. The complex index of refraction was extracted for each layer from measured transmittance and reflectance spectra and from ellipsometry data. The simulations of the transmittance and reflectance spectra are in very good agreement with the measurements. The maximum photocurrent is calculated by convoluting the absorbance of the photoactive film with the solar irradiation spectrum and is in the expected range for dye-sensitized solar cells ($\sim 12 \text{ mA cm}^{-2}$). Preliminary calculations were also made for the CIGS cells alone, where the complex index of refraction was extracted experimentally for each layer using ellipsometry data. The calculated maximum photocurrent is also in the expected range (35 mA cm^{-2}), but the simulations could not yet be validated with experimental data. Simulations of a complete monolithic tandem device show that sufficient light is transmitted to the bottom cell, yielding about 21 mA cm^{-2} (Figure 4). According to the calculation, the current of the top cell limits the device if a CIGS cell with high photocurrent (35 mA cm^{-2}) is used.

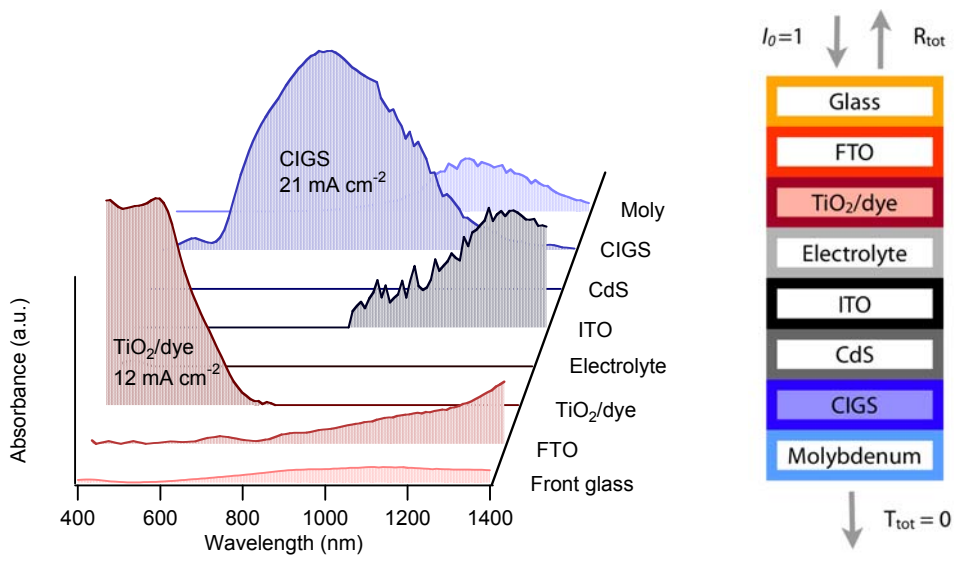


Figure 4. Calculated absorbance in each layer of a monolithic DSC/CIGS tandem cell (right scheme). The sum of the absorbencies and the total reflection adds up to one. From the absorbance one can calculate the maximum photocurrent.

Triple Junction Devices – Preliminary Studies

Last, some preliminary work was carried out on the feasibility of a DSC/CdTe/CIS triple junction solar cells (Figure 5). Theoretically, the absorption characteristics of these materials are close to the band gaps required for an optimized triple junction device. However, the multilayered structure, problems in the interconnection of p-type absorbers with n++ doped TCOs at the back contacts, and bad TCO transmission due to temperature constraints of the finished cells lead to problems in current generation in the bottom cell. As seen in Figure 6, only a small part of the light, about 30 to 40% in the applicable spectral range between 750 and 1200 nm, reaches the bottom cell to generate charge carriers. With these limitations, the bottom cell current density is down to only 3.7 mAcm⁻², while a current density of about 10 mAcm⁻² would be needed to achieve current matching and thus a high efficiency device. However, if all TCO layers could be replaced with high mobility TCOs, such as ITiO, and the problems of interconnections could be overcome, e.g., by the use of p++ doped TCOs, the quoted device structure could be an interesting approach for low-cost high efficiency cells.

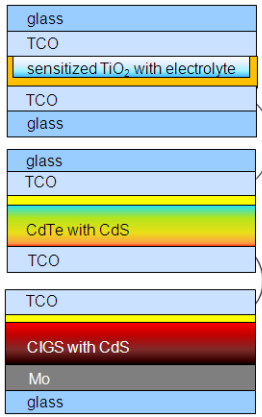


Figure 5: Schematics of a mechanically stacked triple junction DSC/CdTe/CIGS solar cell.

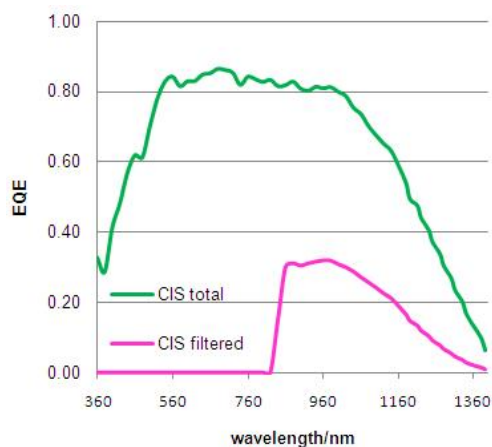


Figure 6: Quantum efficiency of a CIS solar cell under full AM1.5 illumination and after filtering through a DSC/CdTe top stack.

Organic solar cells based on photographic dyes

An important part of this year's research effort was dedicated to the understanding of the basic mechanisms that were still limiting organic solar cells based on cyanine dyes, a special class of photographic dyes. We found that not only charge transport in thin solid cyanine layers, but also charge transfer at both cathode and anode were important factors in limiting device efficiency. After having optimized all three issues, we were able to achieve solar cells based on a cyanine dye donor and a fullerene C_{60} acceptor (see Figure 7) with an external photon to current conversion efficiency of over 80% at maximum. We could therefore show that the commonly used bulk-heterojunction concept used with polymers may not be necessary for thin dye layers with extremely high extinction coefficients. We have secured our finding this year in a Swiss patent application.

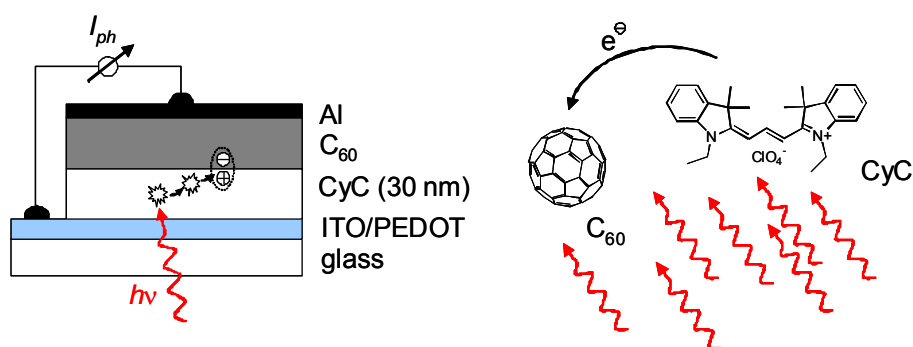


Figure 7: Bilayer organic solar cell consisting of a cyanine donor and a fullerene C_{60} acceptor. The very high absorption coefficient of the cyanine layer allows to use ultrathin layers of 20 nm to 30 nm only that still absorb enough light.

Before organic solar cells based on photographic dyes can be applied in multijunction cell architectures, photosensitivity in the red to near-infrared domain has to be achieved. To explore this possi-

bility, squaraine dyes with extremely high extinction coefficients in the red spectral domain have been applied as thin layers in organic solar cells (Figure 8).

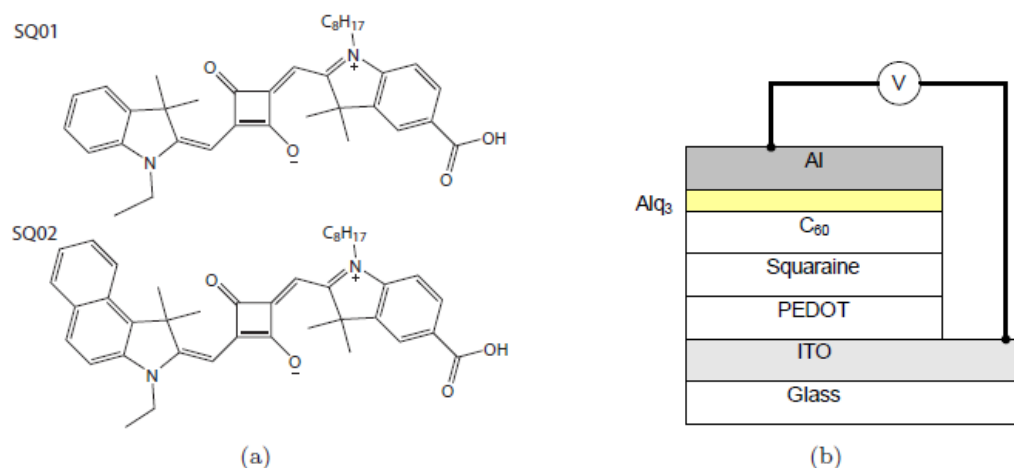


Figure 8 Molecular structure of the squaraine dyes SQ1 and SQ2 used in this study (left). Device architecture (right).

These preliminary devices have shown that photosensitivity in the far red spectral domain can indeed be achieved by using these dyes (Figure 9). The best power conversion efficiency obtained in these preliminary studies arrived at 1%. By applying our competences in charge carrier extraction developed for cyanine dyes, we were recently able to achieve efficiencies over 2% using the same squaraine dyes.

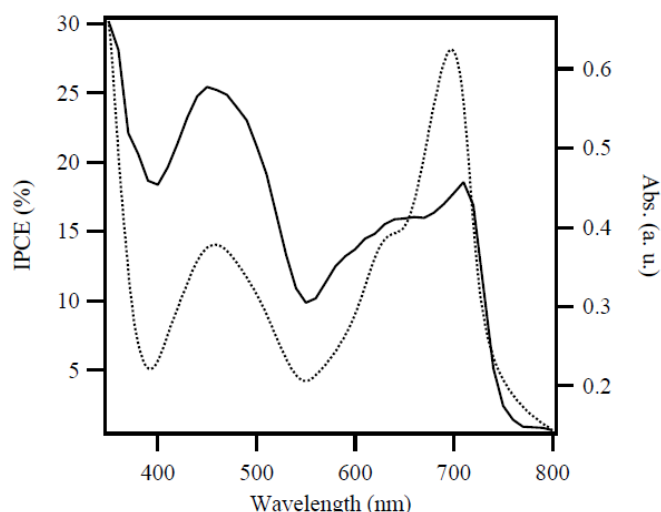


Figure 9 Thin film solar cell absorbance (dotted line) and incident photon to current conversion efficiency (IPCE) of photovoltaic devices based on a 20 nm thick SQ2 donor film and a 40 nm thick fullerene C_{60} acceptor layer.

Outlook Part B

- Future work will focus on blocking the corrosion process with a suitable protective intermediate layer. We plan to test different thin conformal oxide layers deposited by a state-of-the-art *Atomic Layer Deposition* system, which will be installed at the beginning of 2010. In addition we will test the deposition of different spin-coated organic polymers from various solvents.
- Optical modeling of the hybrid tandem device is a valuable additional tool to analyze and optimize the light absorbed in the two subcells. The refractive indices of the layers in the CIGS cell will be characterized more accurately and the output of the optical model will be validated using measured transmittance and reflectance spectra.
- The approach of a triple junction DSC/CdTe/CIS device is a theoretically promising approach. However, efforts are needed to improve the transmission of both the DSC top cell and the CdTe intermediate cell to allow enough light to be transmitted to the bottom cell and to achieve current matching.
- Organic solar cells based on photographic dyes now reach current densities of 8 mA/cm² and are almost ready to be used in multijunction solar cells. In the future, the possibility of using blends of cyanine dyes as electron donors will be investigated in order to broaden the absorption range of these solar cells. Modeling studies will be carried out before starting multijunction device construction.

Thin film photovoltaic device simulation

To perform a complete optoelectronic device simulation of a solar cell one has to consider the light in-coupling into the device structure, the absorption of the photons, the resulting generation of free charge carriers and the extraction of the charge carriers from the device. Improvements were achieved in all these steps. A new measurement setup allows to validate the simulation results.

The ability of the incident light to interfere within the layers of a solar cell structure depends on the coherence length of the input illumination. While the typical thicknesses of the absorbing layers in organic solar cells (on the order of a few hundred nanometers) do not exceed the coherence length of sunlight (on the order of a micrometer), this is however clearly the case for the covering glass or the thick layers encountered in dye-sensitized solar cells. A coherent treatment of such thick layers leads to interference fringes that are not observable in the experiment. To account for the coherence length of the input illumination, the optical device model was extended to allow for an arbitrary configuration of coherent or incoherent layers. Figure 1 illustrates the absorbance for a thin film silicon solar cell for different coherence lengths.

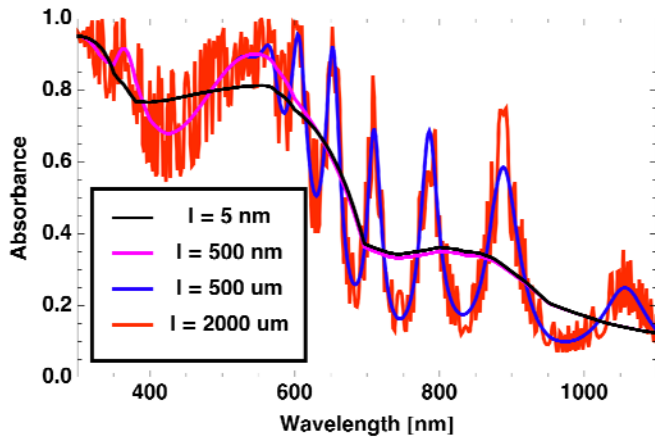


Figure 1: Effect of the coherence length (l) of the input illumination on the absorbance for a thin film silicon solar cell.

The electrical device model has been extended to include charge transfer (CT) excitons. The CT excitons are an intermediary state between the photons and the free charge carriers that are initially generated by the absorption of the photons. The following processes are relevant in the modeling of the CT excitons: First, the absorption of a photon generates a CT exciton. This requires the photon absorption profile that is the result of the optical calculation. Second, free charge carriers (i.e. an electron and a hole) may recombine to generate a CT exciton. The influence of the recombination efficiency that governs this process on the short-circuit current is illustrated in Figure 2. Furthermore there are two processes that describe the depletion of the CT exciton state, namely a decay and a dissociation that produces free charge carriers.

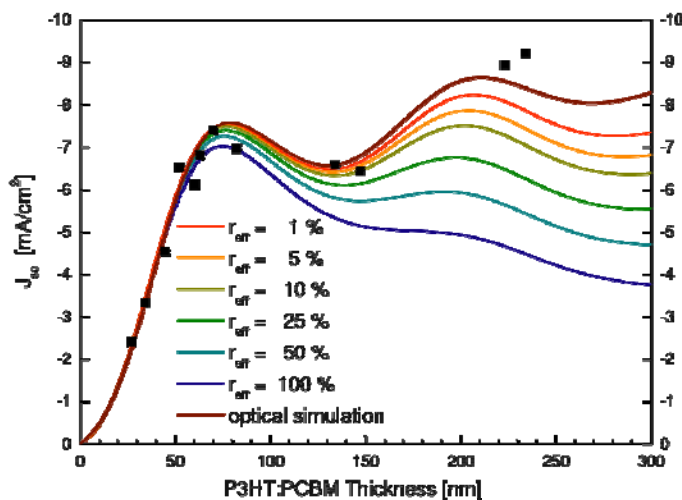


Figure 2: Thickness dependence of the short-circuit current J_{sc} with varying Langevin recombination efficiency r_{eff} . A purely optical simulation is also shown. The simulations are compared with measurements reported by Gilot et al.

To complement and validate the simulation results a new measurement setup has been established that allows for photo-CELIV (charge extraction by linearly increasing voltage) measurements. In these measurements the solar cell is first illuminated by a light flash, after a certain delay time a voltage ramp is then applied to the cell in order to extract the induced charge carriers. The technique allows extracting material parameters such as charge carrier mobilities and lifetimes. Currently the coupled device model is used to examine the validity of the formulas that can be found in the literature for the analysis of photo-CELIV measurements. This should allow a deeper insight into the measurement technique as the simulation gives also access to physical parameters not accessible in the experiment.

5. Publications, Conferences, Patents

Publications

- [1] S. Wenger, S. Seyrling, A. Tiwari, and M. Grätzel, *Fabrication and performance of a monolithic dye-sensitized TiO₂/Cu(In,Ga)Se₂ thin film tandem solar cell*, Applied Physics Letters 94, 173508 (2009).
- [2] S. Seyrling et al.: *Analysis of electronic and optical losses in CIGS/DSC tandem solar cells*. Proceedings of the E-MRS Spring meeting, Strasbourg (2009), submitted for publication, under consideration for special issue of Sol. Energy Mat. Sol. Cells.
- [3] S. Seyrling et al.: *Development of Multijunction Thin Film Solar Cells*. Proceedings of the 34th IEEE Photovoltaic Specialists Conference, Philadelphia (2009), submitted for publication
- [4] R. Bartlome, A. Feltrin, and C. Ballif, "Infrared laser-based monitoring of the silane dissociation during deposition of silicon thin films", Appl. Phys. Lett. **94**, 201501 (2009).
- [5] G. Bugnon, A. Feltrin, F. Meillaud, J. Bailat, and C. Ballif, "Influence of pressure and silane depletion on microcrystalline silicon material quality and solar cell performance", J. Appl. Phys., Vol **105**, 064507 (2009).
- [6] G. Parascandolo, G. Bugnon, A. Feltrin, C. Ballif, "High-rate deposition of microcrystalline silicon in a large-area PECVD reactor and integration in tandem solar cells", Progress in Photovoltaics, *in print*.
- [7] R. Häusermann, E. Knapp, M. Moos, N.A. Reinke, T. Flatz, B. Ruhstaller, "Coupled optoelectronic simulation of organic bulk-heterojunction solar cells: Parameter extraction and sensitivity analysis", J. Appl. Phys., 106, 104507, 2009
- [8] B. Fan, F. A. Castro, J. Heier, R. Hany, F. Nüesch, "High performing doped cyanine bilayer solar cell", *Organic Electronics*. submitted (2009).
- [9] B. Fan, Y. Maniglio, M. Simeunovic, S. Kuster, T. Geiger, R. Hany, F. Nüesch, "Squaraine planar-heterojunction solar cells", *Int. J. Photoenergy*, doi: 10.1155/2009/581068, (2009)

Conferences

- [1] S. Seyrling, S. Bücheler, A. Chirila, J. Perrenoud, R. Verma, S. Wenger, M. Grätzel, and A.N. Tiwari, *Towards the development of high efficiency multijunction thin film solar cells*, Proceedings of the 24th European Photovoltaic Solar Energy Conference and Exhibition, Hamburg, Germany, September 21-25, 2009.
- [2] S. Seyrling, S. Bücheler, A. Chirila, J. Perrenoud, S. Wenger, T. Nakada, M. Grätzel, A.N. Tiwari, *Development of multijunction thin film solar cells*, Proceedings of the 34th IEEE Photovoltaic Specialists Conference, Philadelphia, PA, USA, June 7-12, 2009-
- [3] S. Wenger, S. Seyrling, A. Tiwari, and M. Grätzel, *Optimization of monolithic dye-sensitized TiO₂/Cu(In,Ga)Se₂ thin film tandem solar cells*, Oral presentation at the European Materials Research Society (E-MRS) Spring Meeting, Strasbourg, France, June 8-12, 2009. *E-MRS Young Scientist Award*.

Awarded to a graduate student in recognition of an outstanding paper contributed to the E-MRS Spring Meeting 2009.

- [4] S. Wenger, S. Seyrling, A. Tiwari, and M. Grätzel, *Fabrication and performance of monolithic dye-sensitized $TiO_2/Cu(In,Ga)Se_2$ tandem solar cells*, Poster presentation at the 3rd International Conference on the Industrialization of DSC, Nara, Japan, April 22-24, 2009.
- [5] S. Seyrling et al.: *Towards the Development of High Efficiency Multijunction Thin Film Solar Cells*. Proceedings of the 24th European Photovoltaic Solar Energy Conference, Hamburg (2009), submitted for publication.
- [6] R. Bartlome, B. Strahm, A. Feltrin, and C. Ballif. "Laser-based plasma diagnostics for PECVD of silicon thin films. In Proc. of the 34th IEEE PVSC, Philadelphia, 2009, *in print*.
- [7] B. Strahm, A. Feltrin, R. Bartlome, and C. Ballif, "Optical emission spectroscopy to diagnose powder formation in SiH_4-H_2 discharges", Proc. SPIE, Vol. 7409, 74090E (2009).
- [8] B. Strahm, A. Feltrin, G. Bugnon, F. Meillaud-Sculati, C. Ballif, A. A. Howling, and C. Hollenstein, "Study of the microstructure transition width from amorphous to microcrystalline silicon as a function of the input silane concentration", Proc. SPIE, Vol. 7409, 74090I (2009).
- [9] T. Lanz, B. Perucco, D. Rezzonico, F. Müller, N. A. Reinke, R. Häusermann, B. Ruhstaller, "Optical Simulation of Arbitrary Thin Film Solar Cells with Rough Interfaces", 24th EUPVSEC, 21-25 September 2009, Hamburg, Germany
- [10] S. Wenger, M. Schmid, G. Rothenberger, M. Grätzel, J. O. Schumacher, "Model-Based Optical and Electrical Characterization of Dye-Sensitized Solar Cells", 24th EUPVSEC, 21-25 September 2009, Hamburg, Germany
- [11] N. A. Reinke, R. Häusermann, E. Huber, M. Moos, T. Flatz, B. Ruhstaller, "Fully Coupled Opto-Electronic Modelling of Organic Photovoltaic Cells", HOPV09, 10-13 May 2009, Benidorm, Spain
- [12] R. Häusermann, N.A. Reinke, E. Huber, T. Flatz, M. Moos, B. Ruhstaller, "CT-State Dissociation and Charge Recombination in Organic Photovoltaic Cells", HOPV09, 10-13 May 2009, Benidorm, Spain
- [13] R. Häusermann, N.A. Reinke, E. Huber, T. Flatz, M. Moos, B. Ruhstaller, "CT-State Dissociation and Charge Recombination in OPVs", DPG Spring Meeting, 22-27 March 2009, Dresden, Germany
- [14] N.A. Reinke, R. Häusermann, E. Huber, M. Moos, T. Flatz, B. Ruhstaller, "Fully Coupled Opto-Electronic Modelling of Organic Solar Cells", DPG Spring Meeting, 22-27 March 2009, Dresden, Germany.
- [15] Bin Fan, Roland Hany, Thomas Geiger, Jacques-E. Moser, Frank Nüesch, „Oxidative doping of cyanine/C60 organic solar cells", Solar '09, 10.1.-14.1.2009, Luxor.
- [16] Bin Fan, Jakob Heier, Hadjar Benmansour, Fernando Castro, Thomas Geiger, Roland Hany, Frank Nüesch, „The use of cyanine dyes in solid state organic heterojunction solar cells ", E-MRS, 8.6.-12.6.2009, Strasbourg.
- [17] Bin Fan, Jakob Heier, Hadjar Benmansour, Fernando Castro, Thomas Geiger, Roland Hany, Frank Nüesch, „The Use of Cyanine Dyes in Solid State Organic Heterojunction Solar Cells", MRS Fall Meeting, 30.11.-4.12.2009, Boston.

Patents

[1] U. Kroll and B. Legradic, (2009) *Plasma Processing Apparatus and Method for the Plasma Processing of Substrates*, Patent WO/2009/133189 filed April 2009.

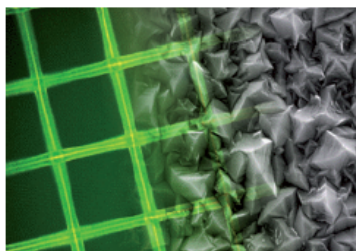
[2] B. Fan, R. Hany, F. Nüesch, *Multi layer organic thin film solar cell*, patent application CH-01475/09.

6. Special events, workshops

- [1] CCEM evaluation meeting on 15.1.2009 at Forum Chriesbach in Dübendorf. Presentation of the goals and achievements of *ThinPV* by Frank Nüesch.
- [2] Presentation on the advancement of *ThinPV* given on 16th May 2009 by Frank Nüesch, Christophe Ballif, Christoph Hollenstein, Beat Ruhstaller at swisselectric research in Bern.
- [3] Presentation of the *ThinPV* project by Frank Nüesch at the Swiss Solar Initiative meeting on August 19th 2009 at Villa Hatt, Zürich.
- [4] *ThinPV* Conference: “Transparent Conducting Electrodes for Photovoltaics” to take place on January 25th in 2010. Organization by Katerina Andric and Frank Nüesch.



Workshop Transparent Conducting Electrodes for Photovoltaics



Stade de Suisse
Bern, Switzerland

Monday, January 25th, 2010

Registration online at
www.empa.ch/tpv

Program

- 09.00 Welcome coffee, registration
- 09.45 Opening
Dr Frank A. Nüesch
Empa, Dübendorf, Switzerland
- 10.00 Degenerate n- and p-type TCO's
Prof. Tadatsugu Minami or
Prof. Toshihiro Miyata,
R&D Center Kanazawa Inst. of Techn., Japan
- 10.30 ZnO electrodes and interfaces for
solar cell applications
Dr Klaus Ellmer
Helmholtz-Zentrum, Berlin, Germany
- 11.00 Fundamentals of high carrier mobility TCO's
Prof. Tobin J. Marks
Northwestern University,
Department of Chemistry, Evanston, USA
- 11.30 Short coffee break
- 12.00 Thermally stable transparent electrodes from
ultra thin metal films for solar cell applications
Prof. Valerio Pruneri
ICFO Inst. De Ciències Fotòniques, Barcelona, Spain
- 12.30 Transparent electrodes based on polymer-
nanotube composites for PV application
Prof. Jonathan N. Coleman
Trinity College, School of Physics,
Dublin, Ireland
- 13.00 Lunch
- 14.30 TCO deposition processes on flexible
polymer films
Dr Matthias Fahlend
Fraunhofer Institut, Dresden, Germany
- 15.00 Use of fabrics for transparent device electrodes
Dr Peter Chabreck
Sefar Division Druck, Thal, Switzerland
- 15.30 Transparent conducting sol-gel ATO coatings
for thin PV device applications
Dr Guillaume Guzman, Corning SA, Avon, France
- 16.00 Laser patterning for thin-film silicon solar modules
Stefan Haas, Forschungszentrum Jülich, Germany
- 16.30 Closure and open discussion
- 17.00 Aperitif

Organisation

- Location Stade de Suisse
Papiermühlstrasse 71, CH-3000 Bern 22
- Date Monday, January 25th, 2010
- Costs Student: CHF 150.- / Scientist: CHF 300.-
- Registration Registration online at
www.empa.ch/tpv
or with the Registration Form
- Registration deadline November 30th, 2009

Conference Office

- Scientific Dr Frank A. Nüesch
Empa
Materials Science & Technology
Oberlandstrasse 129
CH-8600 Dübendorf
Phone: +41 44 823 47 40
Fax: +41 44 823 40 12
E-Mail: frank.nuesch@empa.ch
- Administrative Katerina Andric
Empa
Materials Science & Technology
Oberlandstrasse 129
CH-8600 Dübendorf
Phone: +41 44 823 47 31
Fax: +41 44 823 40 12
E-Mail: katerina.andric@empa.ch
- <http://thinpv.empa.ch>



© Empa 2009/10, Andric, 10

7. Involved Partners

- Institut de Microélectronique, IMT, Neuchâtel (EPFL)
- Centre de Recherches en Physique des Plasmas, CRPP (EPFL)
- Laboratory for Photonics and Interfaces, ISIC, (EPFL)
- Thin Film Physics Group, Technopark Zürich (Empa)
- Laboratory for Functional Polymers, Empa
- Institute of Computational Physics, Winterthur (ZHAW)
- Oerlikon Solar, Trübbach